Accepted Manuscript

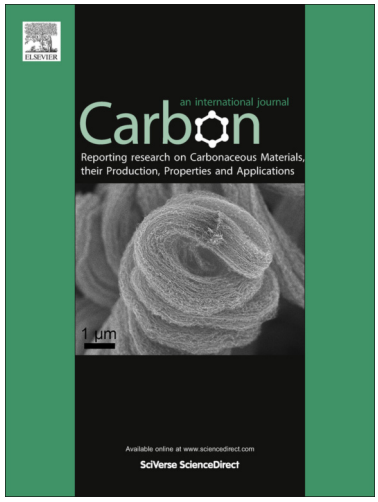

Generation of nitrogen functionalities on activated carbons by amidation reactions and Hofmann rearrangement: chemical and electrochemical characterization

María José Mostazo-López, Ramiro Ruiz-Rosas, Emilia Morallón, Diego Cazorla-Amorós

PII: S0008-6223(15)00380-2
DOI: http://dx.doi.org/10.1016/j.carbon.2015.04.089
Reference: CARBON 9888

To appear in: *Carbon*

Received Date: 30 January 2015
Accepted Date: 26 April 2015

Please cite this article as: Mostazo-López, M.J., Ruiz-Rosas, R., Morallón, E., Cazorla-Amorós, D., Generation of nitrogen functionalities on activated carbons by amidation reactions and Hofmann rearrangement: chemical and electrochemical characterization, *Carbon* (2015), doi: http://dx.doi.org/10.1016/j.carbon.2015.04.089

GENERATION OF NITROGEN FUNCTIONALITIES ON ACTIVATED CARBONS BY AMIDATION REACTION AND HOFMANN REARRANGEMENT. CHEMICAL AND ELECTROCHEMICAL CHARACTERIZATION

María José Mostazo-López[1], Ramiro Ruiz-Rosas[1], Emilia Morallón[2], Diego Cazorla-Amorós[1,*]

[1]Departamento de Química Inorgánica e Instituto Universitario de Materiales. Universidad de Alicante. Apartado 99. E-03080 Alicante. España

[2]Departamento de Química Física e Instituto Universitario de Materiales. Universidad de Alicante. Apartado 99. E-03080 Alicante. España

[*]Corresponding author: Tel. +34965903946. E-mail: cazorla@ua.es

Abstract

Nitrogen functionalization of a highly microporous activated carbon (BET surface area higher than 3000 m^2/g) has been achieved using the following sequence of treatments: (i) chemical oxidation using concentrated nitric acid, (ii) amidation by acyl chloride substitution with NH_4NO_3 and (iii) amination by Hoffman rearrangement. This reaction pathway yielded amide and amine functional groups, and a total nitrogen content higher than 3 at%. It is achieved producing only a small decrease (20%) of the starting microporosity, being most of it related to the initial wet oxidation of the activated carbon. Remarkably, nitrogen aromatic rings were also formed as a consequence of secondary cyclation reactions. The controlled step-by-step modification of the surface chemistry allowed to assess the influence of individual nitrogen surface groups in the electrochemical performance in 1M H_2SO_4 of the carbon materials. The largest gravimetric capacitance was registered for the pristine activated carbon due to its largest apparent surface area. The nitrogen-containing activated carbons showed the highest surface capacitances. Interestingly, the amidated activated carbon showed the superior capacitance retention due to the presence of functional groups (such as lactams, imides and pyrroles) that enhance electrical conductivity through their electron-donating properties, showing a capacitance of 83 F/g at 50 A/g.

1. INTRODUCTION

Surface chemistry plays a major role in determining the physicochemical properties of carbon materials. It highly relies on the presence of functionalities from different heteroatoms (i.e. oxygen and nitrogen, and some others in lesser amounts), either linked to the carbon surface or introduced inside the carbon atom framework. Along with their structural and textural properties, surface chemistry dictates the potential use of carbon materials in a wide variety of applications in the fields of catalysis, energy storage, environmental protection and biomedicine [1-3]. More particularly, nitrogen functionalities in porous carbon materials modifies their electronic and the electrochemical reactivity properties and confer basic character to the carbon surface, enhancing the interaction with acid molecules [4]. Consequently, the production of nitrogen-containing porous carbon materials have raised a great interest due to their promising performance as electrocatalysts for the oxygen reduction reaction in fuel cells [5], as electrodes for supercapacitors [6-8] and as adsorbents for the capture of acid gases [9,10].

Nitrogen-containing porous carbons are usually synthesized by two methodologies: reaction of the material with a nitrogen-containing reagent (NH_3, HCN, etc) or carbonization/activation of nitrogen-rich carbon precursors (urea, melamine, polyaniline, etc.) [4,6,7]. The surface chemistry of the corresponding material depends on the treatment conditions, which includes the nature of the selected precursor/reagent and the treatment temperature. Hence, direct synthesis requires the use of high temperatures (over 600º C) which does not allow to control the type of functional groups that are formed on the carbon material. Similarly, post-treatments with gaseous reagents are usually conducted at high temperatures, though other approaches at low temperatures (under 600º C) are found to be interesting for attaining different functional groups, such as amides [11] or imides [6].

Post-treatment through organic reactions can be a quite interesting approach because they permit the use of soft treatment conditions that may preserve the structural characteristics of the carbon materials, and provide different reaction pathways for finely tuning the surface chemistry with a wide variety of surface groups [12-19]. Nitrogen functionalization is usually achieved through the oxidation of the carbon material with HNO_3 in order to generate carboxylic acids on its surface, which acts as the anchorage points for the subsequent reactions [6, 18]. They can directly react with nitrogen-containing reagents to attach this heteroatom onto the surface, but when this material is previously treated with $SOCl_2$ the

amount of nitrogen introduced in the carbon material is higher [16]. When this reaction is conducted using amines as the nitrogen-containing reagent, it produces an amide group substituted with an aliphatic chain, which can block the microporosity depending on the size of the hydrocarbon chain of the amine used as reagent [16]. However, when the amine is directly attached to the surface [19] or a primary amide is produced instead of a secondary one, the blocking of porosity might be lower. Also, primary amides can be converted to amines directly anchored to the carbon surface by Hofmann rearrangement that has been proven to work with SWCNTs [20].

Interestingly, the selectivity of the synthetic route towards the desired amides or amines is not usually very high due to the complex surface chemistry of the carbon materials. For these reasons, in this work we study the modification of the surface chemistry of a superporous activated carbon with the introduction of N functional groups through organic reactions schematized in Figure 1. The modification approach consists in: (I) chemical oxidation with HNO_3 for the generation of carboxylic acids (KUA-COOH); (II) amidation treatment by introduction of acyl chloride functionalities and conversion of these groups into amide groups (KUA-$CONH_2$); (III) transformation of amides into amine groups by Hofmann rearrangement (KUA-NH_2). The porous texture, surface chemistry and electrochemical properties in aqueous electrolyte of all the obtained materials will be analyzed, trying to understand the reactions occurring that may explain the structural changes of the functional groups introduced on the carbon material surface.

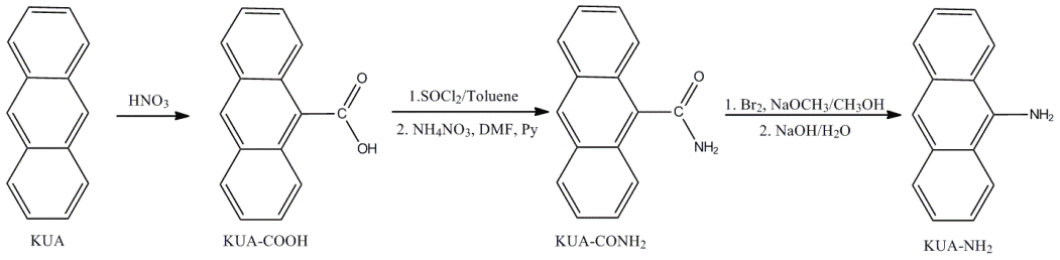

Figure 1. Chemical route used for the modification of the activated carbon KUA: (a) chemical oxidation with HNO_3 (KUA-COOH), (b) $SOCl_2$ treatment and amidation (KUA-$CONH_2$) and (c) amination (KUA-NH_2).

2. EXPERIMENTAL

2.1. Activated carbon

A highly microporous activated carbon prepared in our laboratory has been used as the starting material for nitrogen incorporation via organic chemical modification. The pristine material, henceforth named KUA, has been obtained by chemical activation of an anthracite with KOH using an impregnation ratio of activating agent to raw material of 4:1 and an activation temperature of 750º C under inert atmosphere, which was held for 1 hour. More details about the preparation process are available elsewhere [21].

2.1.1. Chemical oxidation with HNO_3

The chemical oxidation of the activated carbon KUA was done using HNO_3 as oxidant. Nitric acid is known as strong oxidizing agent that yields an important amount of carboxylic acids when used for treating carbon materials, and it has been widely used in literature for oxygen surface functionalization [22-24].

The oxidation treatment has been adopted from previous studies of our research group [24]. Briefly, 1g of activated carbon (KUA) was contacted with 40mL of HNO_3 65 wt% under stirring during 3 hours at room temperature. After that, KUA-COOH was filtrated and washed with Milli-Q water until the pH of elution was neutral. Finally, the sample (named KUA-COOH) was dried at 100º C.

2.1.2. Generation of amide functionalities

The amidation process consists in two sequential steps: first, acyl chlorides are generated from carboxylic functionalities and, secondly, a nitrogen-containing compound is anchored to the carbonyl via nucleophilic substitution over the acyl chloride. These reactions were carried out inside a Schlenk system. The acyl chloride formation is accomplished as follows [25]: Dry KUA-COOH (1 g) was introduced in a round bottom flask with 50 mL of toluene and 5 mL of $SOCl_2$ was added to the flask. The mixture was refluxed at 120ºC for 5 hours under Ar atmosphere. After that time, the sample was washed with toluene and dried under vacuum for 14h.

The reaction for the generation of the amide group has been adapted from that proposed by Gromov and coworkers for CNTs [20]. KUA-COCl was added into a 2M NH_4NO_3/DMF solution (activated carbon to solution ratio of 1g/300mL) in a round bottom flask. Then, 300 mL of pyridine were added slowly to the round bottom flask under continuous stirring at room temperature. The mixture was stirred at 70 ºC for 65 hours under Ar atmosphere. The obtained amidated sample (KUA-$CONH_2$) was washed with abundant water and ethanol,

filtered and dried at 100º C overnight. It can be seen that the proposed approach uses harmful and toxic products, which renders unadvisable its direct use for large scale functionalization of activated carbons. It is also possible to use different reactions for the formation of amide bridges over the surface carbon materials [26]. Nonetheless, the selected synthesis ensures a high functionalization degree, allowing a clear assessment of the extent and nature of the surface chemistry modification. Afterwards, the proposed reaction pathway can be used as the starting point for the development of greener, simpler and less energy- and time-demanding (i.e. "softer") procedures for functionalization of activated carbon using organic chemistry reactions, as in the case of ongoing research in our laboratory.

2.1.3. Generation of amine functionalities

Amine functionalization was carried out using a Hofmann rearrangement in the previously attached amides [20]: 10 mL of Br_2 was added into a solution of 3% wt. $NaOCH_3$ in CH_3OH. KUA-$CONH_2$ (0.5 g) were added to that solution, and the mixture was stirred at 70º C for 4 hours. Then, additional 4 mL Br_2 were added, and the mixture was stirred for 20 hours at 70º C. The product was isolated by filtration, washed with saturated Na_2CO_3, water and ethanol. The aminated activated carbon was obtained after hydrolyzing the recovered sample in 500 mL of 0.1M NaOH for 24 hours, washing with water, and finally filtering and drying the sample at 100º C overnight. This activated carbon is named KUA-NH_2.

2.2 Electrochemical characterization

Carbon electrodes for electrochemical characterization were prepared by mixing the activated carbon with acetylene black and polytetrafluoroethylene (PTFE) as binder in a ratio of 90:5:5 (w/w). The total weight of the electrode was ~9 mg (dry basis). For shaping the electrodes, a sample sheet was cut into a circular shape with an area of 1.2 cm^2 and pressed for 5 min at 2 tons to guarantee a homogeneous thickness. After that, the electrode was placed on a gold disk used as a current collector. The electrodes were impregnated for 2 days into 1M H_2SO_4 previously to electrochemical measurements.

The electrochemical characterization was performed by using an Autolab PGSTAT302 for cyclic voltammetry and Arbin SCTS for galvanostatic charge-discharge cycles. The electrochemical characterization of the different materials synthesized was performed by using a three-electrode configuration. As counter electrode, more than 20 mg of a KUA electrode was used. Both electrodes were placed against each other and separated by a nylon

membrane (pore size: 320 nm). Ag/AgCl/KCl (3M) was used as reference electrode in all cases. 1M H_2SO_4 was used as aqueous electrolyte. The electrochemical performance of all samples was tested by CV at sweep rates between 1 and 50 mV/s and galvanostatic charge-discharge (GCD) cycles at current densities of 50-50000 mA/g. The potential range used for all the measurements was 0.2-0.8 V vs Ag/AgCl/KCl (3M). CV capacitance was calculated from the area of the voltammogram, while GCD capacitance was obtained using the next equation:

$$C_g = \frac{j \cdot t}{\Delta V}$$

Where j is the specific current (A/g), t is the discharge time and ΔV is the difference of potential (0.6 V in all experiments). The results are expressed in F/g, taking into account the weight of the active material of the electrode.

2.3. Porous texture and surface chemistry characterization

The porous texture characterization was carried out by N_2 adsorption-desorption isotherms at -196º C and by CO_2 adsorption at 0º C by using an Autosorb-6-Quantachrome apparatus. The samples were outgassed at 200º C for 4 hours before the experiments. The apparent surface area was obtained from N_2 adsorption-desorption isotherms by using the BET equation. The micropore volume was determined by Dubinin-Radushkevich method applied to the CO_2 and N_2 adsorption isotherms.

The surface chemistry of the samples was analyzed by TPD and XPS. TPD experiments were performed by heating the samples (~10 mg) to 950º C (at a heating rate of 20º C/min) under a helium flow rate of 100 mL/min. The analysis were carried out by using a TGA-DSC instrument (TA Instruments, SDT Q600 Simultaneous) coupled to a mass spectrometer (Thermostar, Balzers, BSC 200). X-ray Photoelectron Spectroscopy (XPS) analyses were carried out using a VG-Microtech Multilab 3000 spectrometer, equipped with an Al anode. The deconvolution of N1s spectra was carried out by using Gaussian functions with 20% of Lorentzian component. FWHM of the peaks was kept between 1.3 and 1.5 eV and a Shirley line was used for estimating the background signal.

3. RESULTS AND DISCUSSION

3.1. Porous texture characterization

Figure 2 shows the N_2 adsorption-desorption isotherms for the original activated carbon and the activated carbon at different stages of the proposed surface chemistry modification protocol. It can be seen that nitrogen uptake in KUA mainly occurs at low relative pressures, showing type I isotherm, characteristic of a microporous material. The wide knee observed in the isotherm at low relative pressures indicates that the material has a wide micropore size distribution. Both characteristics of the nitrogen isotherm are also observed for all the modified activated carbons, although the nitrogen uptake seems to be affected differently by each chemical treatment.

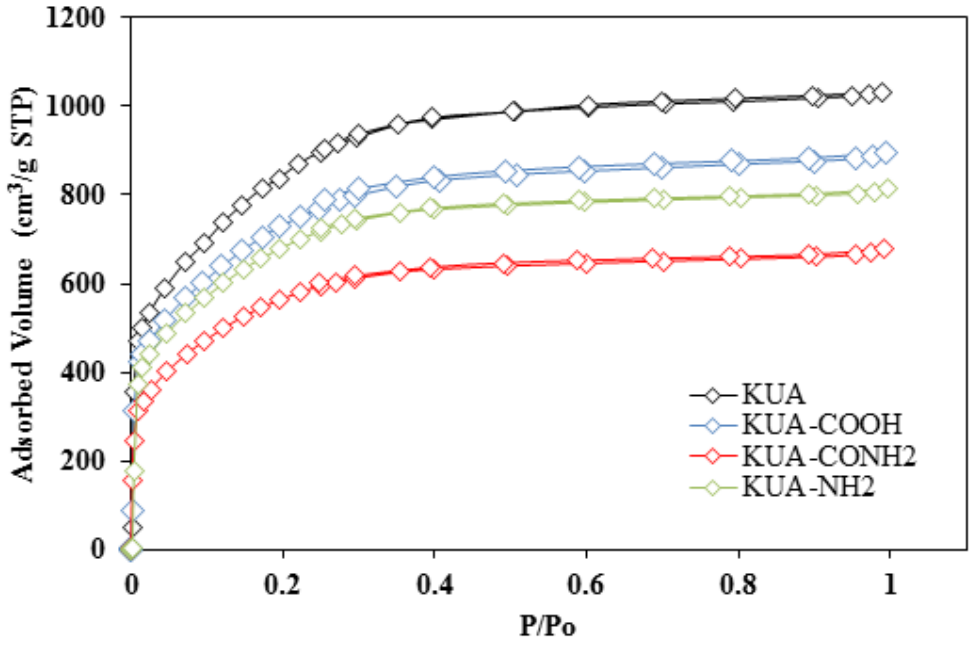

Figure 2. N_2 adsorption-desorption isotherms of the activated carbons KUA, KUA-COOH, KUA-$CONH_2$ and KUA-NH_2.

Table 1 summarizes the porous texture for all the activated carbon samples. The pristine activated carbon (KUA) presents a large apparent surface area. The micropore volume determined by CO_2 adsorption at 0º C ($V_{DR}^{CO_2}$) corresponds to the volume of the narrowest micropores (<0.7 nm), while the obtained by N_2 adsorption at -196º C ($V_{DR}^{N_2}$) corresponds to the whole microporosity (<2nm) [27]. The higher micropore volume measured by nitrogen adsorption indicates that the activated carbon presents a wide micropore size distribution.

Table 1. Textural properties and XPS elemental surface composition for the pristine and modified activated carbons.

Sample	S_{BET} (m^2/g)	$V_{DR}^{N_2}$ (cm^3/g)	$V_{DR}^{CO_2}$ (cm^3/g)	C_{XPS} (at.%)	O_{XPS} (at.%)	N_{XPS} (at.%)
KUA	3140	1.10	0.56	90.9	8.8	0.3
KUA-COOH	2680	0.96	0.45	81.8	18.2	-
KUA-$CONH_2$	2080	0.74	0.44	84.2	12.0	3.8
KUA-NH_2	2450	0.91	0.42	79.1	17.9	3.0
KUA-$CONH_2$_T950	-	-	-	94.5	4.4	1.1
KUA-NH_2_T950	-	-	-	89.9	8.8	1.3

The sample KUA-COOH showed a decrease in the nitrogen uptake, in the apparent surface area and in the pore volume (Figure 2 and Table 1). This effect is related to the generation of surface groups that can occupy the entrance and some volume of the microporosity [23, 24]. In the case of KUA-$CONH_2$, the amidation treatment produced a further decrease of $V_{DR}^{N_2}$, whereas $V_{DR}^{CO_2}$ remains invariable. This decrease suggests that the modification of the surface chemistry involves the largest micropores, while the narrowest microporosity is probably not accessible to the reagents.

The amination treatment leaded to an increase of the specific surface area and $V_{DR}^{N_2}$ of KUA-NH_2 when compared to KUA-$CONH_2$ sample (Table 1 and Figure 2). The narrowest microporosity remains again practically invariable. If we assume that the desired reaction has been carried out, the size of the functional groups that occupy or block the microporosity in KUA-NH_2 should be smaller than those in KUA-$CONH_2$, because of the loss of a CO molecule in the production of amines from amides. This means that the change in the microporosity is in agreement with the intended functionalization of the activated carbon sample.

3.2. Surface chemistry characterization

3.2.1. XPS

Table 1 compiles the composition of the surface chemistry of the samples obtained by XPS. The pristine activated carbon (KUA) is composed mainly by carbon and a relatively high amount of oxygen. XPS analysis of KUA-COOH confirms that the oxidation of this material has been produced during the treatment with HNO_3. The same technique also corroborates that nitrogen is attached onto the surface of the activated carbon KUA-$CONH_2$, remaining on it after completing the treatment for amination (KUA-NH_2). It is important to highlight that more than 3 at.% nitrogen content has been successfully loaded onto the carbon surface while

producing only a minor change of the porous texture of the activated carbon (less than 5% when BET surface area of KUA-COOH and KUA-NH_2 are compared, Table 1). This is a remarkable result since maintaining the porosity of the material is of huge importance for all the surface-dependent applications of nitrogen-doped porous carbons. In comparison, other amidation reactions over activated carbon produced a loss of specific surface area of 42% and 90%, depending on the amine used as reagent in the amidation reaction [16]. The results indicate that the amidation procedure proposed in this work is less detrimental to the porous texture than other approaches involving larger amines.

The oxygen amount measured in each step (Table 1) can also give some information about the process responsible for the nitrogen functionalization. After the amidation step, the introduction of nitrogen is accompanied by a consumption of oxygen, which evidences that the attachment of nitrogen to the surface has been produced mainly through oxygen functional groups. On the other hand, the sample KUA-NH_2 presents an oxygen content similar to KUA-COOH (18%, approximately), and it has also been confirmed by TPD measurements, see section 3.2.2. This result is initially unexpected, because this step might lead to the loss of CO of the amide group through a rearrangement and decarboxylation, in order to obtain amine functionality, so that some loss of oxygen should happen. This increase is probably related to a collateral oxidation during the amination treatment. This will be explained later in more detail. The amount of residual bromine containing species has been determined to be 0.1% at., and therefore are not considered to be relevant in the electrochemical performance of KUA-NH_2.

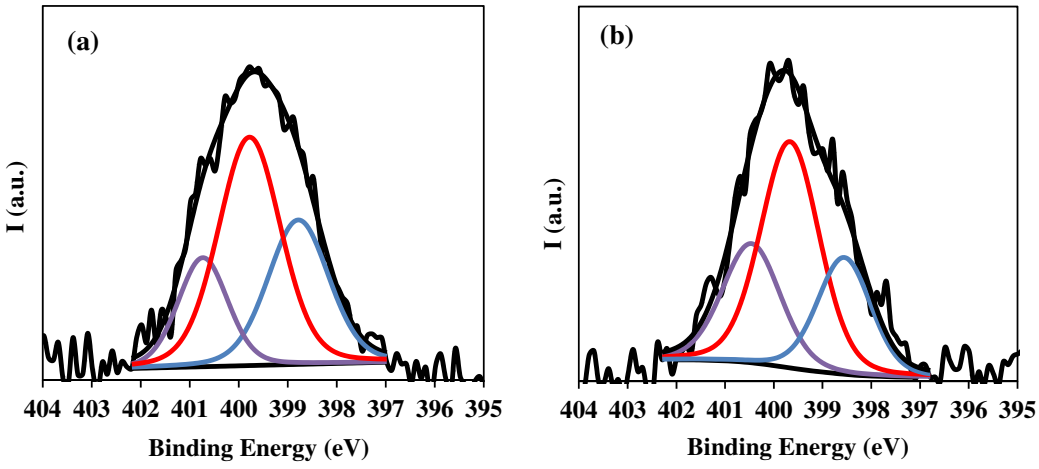

Figure 3. N1s XPS deconvolution of (a) KUA-$CONH_2$, (b) KUA-NH_2.

Figures 3a and b show the N1s XPS spectra of the samples KUA-$CONH_2$ and KUA-NH_2. They have been deconvoluted according to the literature [9,14,28-32]. Table 2 summarizes the results of the XPS analysis. The spectra of both samples revealed the existence of at least three species with different binding energies. In the case of KUA-$CONH_2$, the spectrum can be separated into three peaks located at 400.7, 399.8 and 398.8 eV. The peak at 399.8 eV is assigned to amides, amines, lactams and imides on the surface [30]. The formation of lactams and imides during amidation is plausible from already formed amides groups, since they can condense with adjacent hydroxyls and carboxylic acids that were already over the carbon surface or that can be formed during the initial stages of the wet acid oxidation of the surface. In this sense, the generation of these species could take place from anhydrides [33] and lactones [34], as is showed in Figures 4a and 4b. Similar paths have been proposed for the treatment of non-porous carbon materials with NH_3 gas [6]. At this stage of the modification protocol, the presence of amines should be discarded because their formation could not be explained from the expected reactions; however, it is not possible to discard its presence with the information obtained by XPS.

Table 2. Assignment of N1s deconvoluted curves to nitrogen functional groups.

Sample	Binding Energy (eV)	Functional Group	N (at. %)	Relative %
KUA-$CONH_2$	400.7 ± 0.2	Pyrrole, pyridone	0.72	19
	399.8 ± 0.2	Amide, Lactam, Amine, Imide	1.89	50
	398.8 ± 0.2	Pyridine, Imine	1.17	31
KUA-NH_2	400.5 ± 0.2	Pyrrole, Pyridone	0.72	27
	399.6 ± 0.2	Amide, Lactam, Amine, Imide	1.25	48
	398.5 ± 0.2	Pyridine, Imine	0.65	25
KUA-$CONH_2$ after TPD	398.4 ± 0.2	Pyridine	0.55	49
	400.6 ± 0.2	Pyrrole, Pyridone	0.57	51
KUA-NH_2 after TPD	398.3 ± 0.2	Pyridine	0.42	31
	400.2 ± 0.2	Pyrrole, Pyridone	0.92	69

The peak at 400.7 eV in the N1s spectra of KUA-$CONH_2$ (400.7 eV) is assigned to pyrrole and pyridone functional groups, while that found at 398.8 eV is associated to the presence of pyridines and imines [9,28,30,32]. The presence of adsorbed pyridine or DMF, which could cause misleading XPS assignments, has been ruled out by following the 52 and 42 m/z signals during the TPD experiments which did not show any change with respect to the background. The formation of nitrogen heterocycles at such a low temperatures is an unexpected outcome of the proposed surface modification protocol. This striking result can be explained taking into account the heterogeneity of the activated carbon surface and the availability of different surface oxygen groups. Pyridone can be formed from amide groups when they condense with adjacent hydroxyls in order to produce lactams, which are tautomers of pyridone (Figure 4c) [31,35]. As for the pyiridines/imines, the imines can be generated by reaction between a carbonyl group (aldehyde or ketone) and a nitrogen reactant, such as secondary/tertiary amines and ammonia according to the literature [36,37]. The imines obtained from the last one are more stable when they are linked to two carbons forming an aromatic ring (i.e pyrroles) [37] rather than in form of terminal imines; nevertheless both of them could coexist in the carbon surface. A possible reaction pathways for the formation of imines and pyrroles are shown in Figures 5a and 5b.

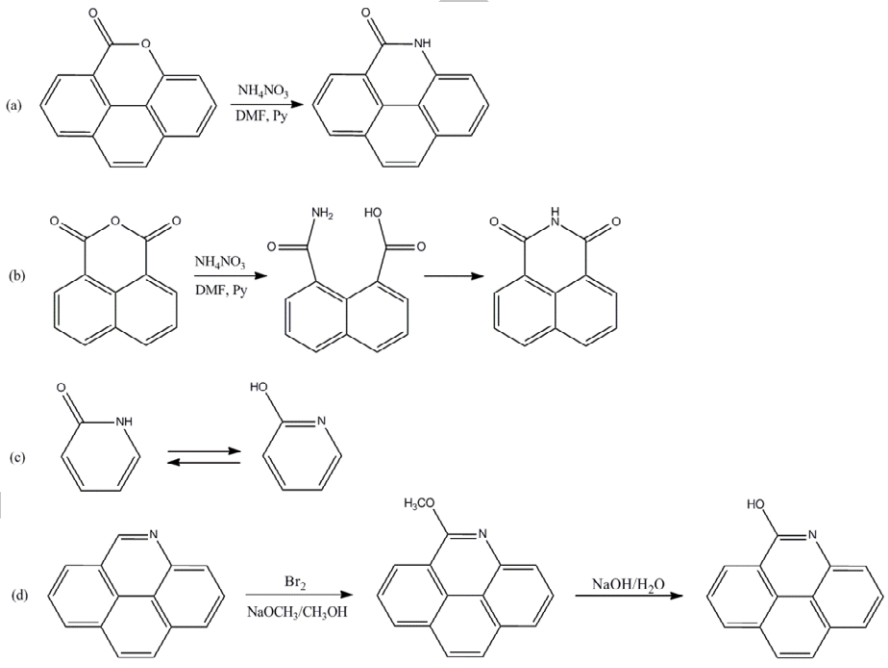

Figure 4. (a) Formation of lactams from lactones; (b) formation of imides from anhydrides; (c) tautomerization equilibrium of the functional groups lactam (left) and pyridone (right); (d) formation of pyridones from pyridines.

When the imines are formed, condensation reactions with aldehydes and ketones can take place, and nitrogen aromatic heterocycles would be produced [38], which structure will depend on the distance between the carbonyls. Hence, two carbonyls separated by two carbon atoms allow the formation of cycles of five members (pyrrole), Figure 5b, whilst a distance of three carbon atoms, Figure 5c, entails the production of six member rings (pyridine). The condensation required to form a heterocycle implies the loss of two H_2O molecules. It should be pointed out that the formation of aromatic rings requires the formation of an intermediate (enamines), as illustrated in Figure 5. The atomic composition measured by XPS seems to validate this hypothesis. The oxygen amount diminishes in 6.2 at.% after the amidation treatment, whereas the oxygen consumption expected from the amount of freshly formed amides and heterocycles is 5.7 at.%, according to the reactions proposed in Figures 4 and 5.

The analysis of the N1s spectra of KUA-NH_2 shows significant changes in comparison with KUA-$CONH_2$. Both samples present peaks with similar binding energies, as can be confirmed in Table 2, but their distribution is different. The peak at 399.6 eV should be associated to the presence of amines on the surface [30,32]. Nevertheless, this assignment is not enough to confirm the formation of amines from amides, since both functional groups appear in the same range of binding energy, according to the literature. On the other hand, the peaks at 400.4 and 398.5 eV can be assigned to the functional groups formed following the reactions showed in Figure 5, as in the case of KUA-$CONH_2$. However, in the sample KUA-NH_2 there exists a larger relative amount of species of high binding energy (pyrroles and/or pyridones), Table 2.

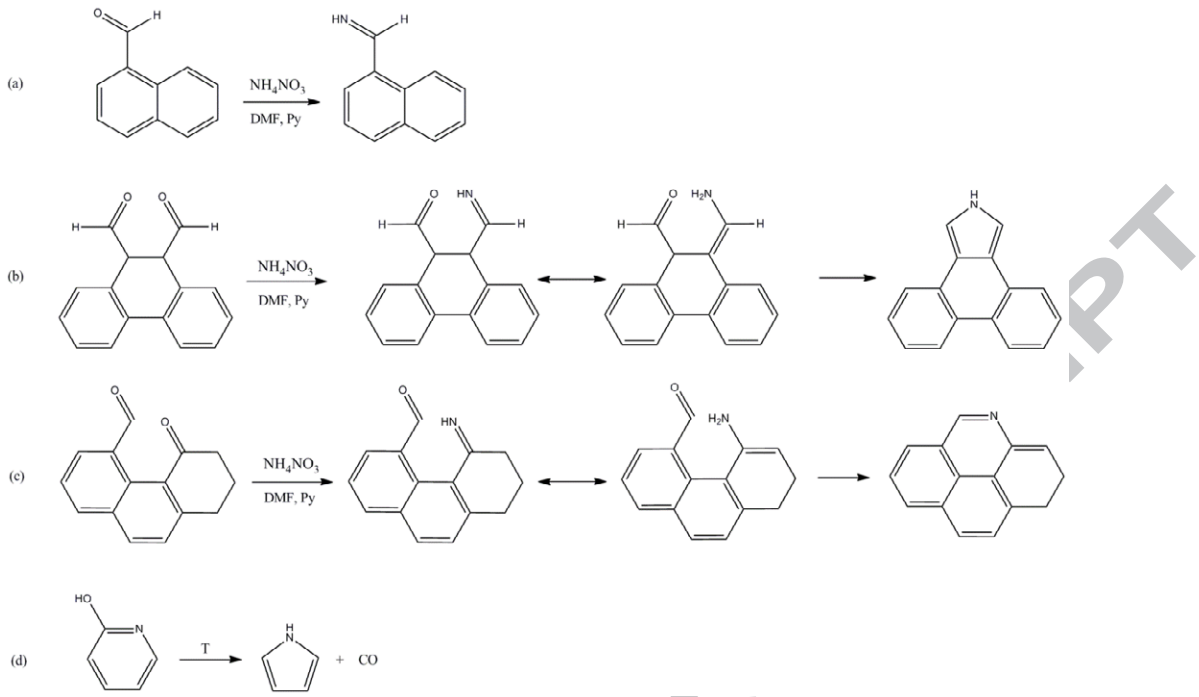

Figure 5. Formation of (a) imines, (b) pyrroles and (c) pyridones from aldehydes and ketones; (d) thermal decomposition of pyridone to form pyrrole through loss of a CO group.

The increase in the oxygen amount detected by XPS and TPD after amination indicates that other reactions have taken place in addition to the conversion of amides to amines. This is confirmed when the step c in Figure 1 is directly applied to KUA-COOH. These results proved that the attachment of methoxide and/or hydroxyl groups occurs onto the surface of KUA-NH_2 and that it takes place through substitution reactions without any further oxidation. This can also be related to the larger relative amount of N-functional groups at 400.4 0.2 eV in this sample in comparison with KUA-$CONH_2$. A possible explanation is the nucleophilic substitution during the reaction in the adjacent position of the nitrogen on the pyridine rings (Figure 4d). Under this hypothesis, the methoxide present in the media during the first step of the reaction, or the hydroxide ions present in the second step, could be attached to the adjacent carbon of the nitrogen group due to the influence of the latter, which confers π deficient character to the ring [35]. This process could also happen sequentially: first, attachment of methoxide into the pyridine ring and secondly, the substitution of methoxide by hydroxide ions, as is shown in Figure 4d. Hence, the substitution in 2 position of pyridine would generate pyridones, so that the amount of groups at the binding energy of 400.4 eV would increase as well as the oxygen content.

Finally, the decrease of nitrogen content in KUA-NH_2 (Table 1) can be associated to the hydrolysis of imines to carbonyls (explaining the decrease of the peak at 398.5 eV, Table 2), which is favored in acid media [37], but that can also happen easily in water [39]. As for the decrease detected at 399.5 eV, it can be related to the loss of part of the amides and their derivatives of the KUA-$CONH_2$, since amines are stable in the preparation conditions.

3.2.2. Temperature Programmed Desorption

Table 3 reports the amount of CO and CO_2 desorbed, as well as the total oxygen amount (calculated as CO + $2CO_2$) during the TPD experiments for all the studied samples. It can be appreciated that the tendencies in the amount of total oxygen for each preparation step coincide with those obtained by XPS (Table 1). Differences in the obtained amounts are due to the techniques being not quantitatively comparable. XPS gives information about the most external surface of the sample; while the oxygen amount obtained from TPD analyses is usually underestimated, since some oxygen functional groups can thermally decompose forming water, which has not been quantified, or can decompose at temperatures higher than those reached at the end of the TPD experiment.

Table 3. Amount of evolved CO, CO_2 and total O obtained from the TPD experiments.

Sample	CO (µmol/g)	O_{CO} (wt. %)	CO_2 (µmol/g)	O_{CO2} (wt. %)	O (µmol/g)	O (wt. %)
KUA	2100	3.4	500	1.6	3100	5.0
KUA-COOH	4030	6.5	1680	5.4	7390	11.8
KUA-$CONH_2$	2490	4.0	1030	3.3	4550	7.3
KUA-NH_2	2800	4.5	1480	4.7	5760	9.2

Figure 6 shows the CO and CO_2 TPD profiles for the pristine and surface-modified activated carbons obtained after each synthesis step. The pristine sample (KUA) presents a remarkable variety of oxygen groups on its surface, all of them generated during the activation process. Its aimed surface functionalization with carboxylic acids seems to be accomplished after the nitric acid treatment, as pointed out by the large amount of CO_2 desorption observed between 200 and 400ºC as consequence of the decomposition of carboxylic acids [22, 40-42]. Collaterally, the amount of desorbed CO, which in pristine KUA sample results from the

decomposition of carbonyls and quinones (CO at temperatures over 700ºC) and as phenols (related to CO evolution at 600-700ºC) in a lower extent [40], have also increased after the nitric acid oxidation. Some CO desorption at temperatures lower than 600ºC is observed because of the presence of anhydride groups, being their amount also higher for the KUA-COOH sample. These groups thermally decompose as CO and CO_2, thus the CO desorption is accompanied by CO_2 evolution in similar amounts at temperatures between 400 and 600ºC. The results from the nitric acid treatment are in line with previous studies from our research group [24,43] and the abundant literature regarding wet oxidation of porous carbons [23, 44].

Furthermore, the comparison between the profiles from the oxidized and the amidated and aminated samples in Figure 6 allows us to clarify both the changes in the surface oxygen groups produced during the different steps of the functionalization and the most probable mechanism for the formation of the nitrogen groups. The functionalization with nitrogen groups during amidation is produced through substitution and condensation reactions onto surface oxygen groups, as pointed out by the lower CO_2 and CO (at high temperatures) evolutions measured for the KUA-$CONH_2$ sample if compared to that of KUA-COOH. More concretely, the comparison of the CO_2 profiles evidences consumption of carboxylic acids (300ºC) and lactones (350-600ºC), as can be observed in Figure 6a (total consumed amount being 650 μmol/g). This decrease is expected according to the desired reaction, since the formation of amide groups and its derivatives requires the consumption of CO_2-desorbing groups (see Figure 1). On the other hand, the KUA-$CONH_2$ sample shows a decrease in the evolution of CO groups at high temperatures, Figure 6b, that is quantified to be 1500 μmol/g. This consumption of CO groups is related to the formation of another type of nitrogen functional groups (Figures 5a, b and c) that, taking into account the results obtained by XPS, might be imines, pyrroles, pyridones and pyridines.

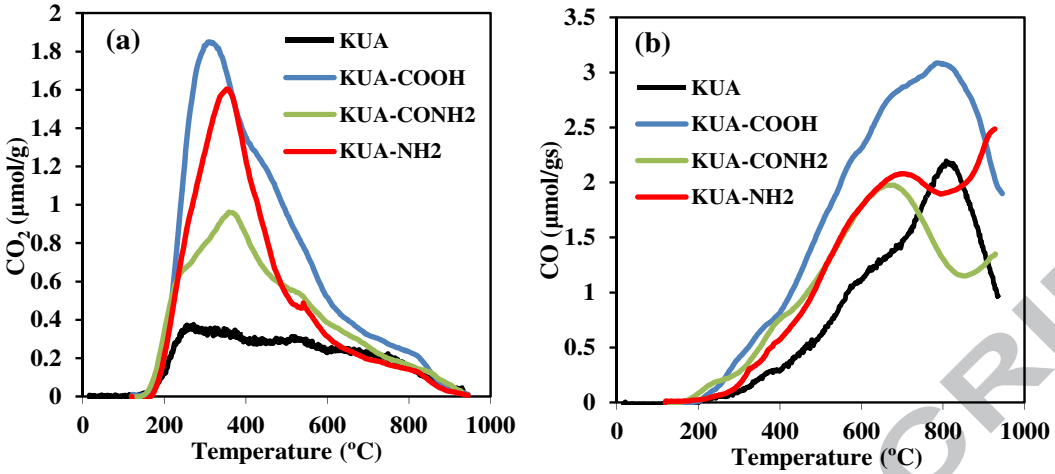

Figure 6. Comparison between (a) CO_2 and (b) CO TPD profiles of KUA-COOH, KUA-$CONH_2$ and KUA-NH_2.

Further evidences of the attained nitrogen functionalization have been obtained during the TPD experiments. Indeed, Figure 7a, which presents the m/z=14 signal (arbitrary units) as a function of temperature for the TPD of KUA-$CONH_2$, shows a peak at 380º C that is related to the evolution of a nitrogen-containing molecule. It also coincides with a CO desorption shoulder (Figure 6b), providing enough evidences of the decomposition of the amide group. Furthermore, the continuous N desorption along the whole temperature range is probably due to lactams decomposition, which can either desorb at higher temperatures or react forming pyridines, and the degradation of aromatic rings (pyrroles, pyridones and pyridines) at even higher temperatures [30]. This is confirmed by the XPS experiments obtained for the samples thermally treated until 950 ºC, Table 2, where an important decrease in the N content is detected and only contributions of pyrrole/pyridone and pyridines are observed.

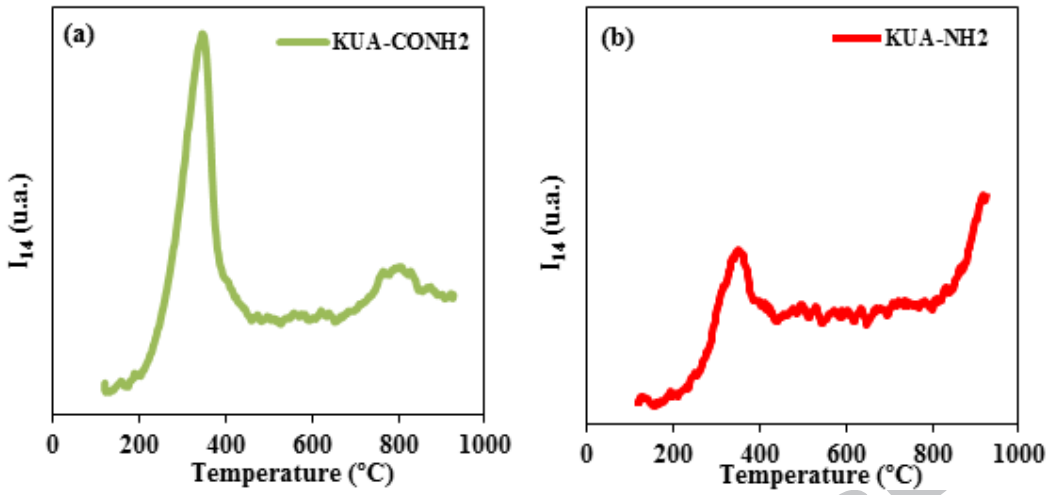

Figure 7. I14 signal during TPD experiment for (a) KUA-$CONH_2$ and (b) KUA-NH_2 samples.

Additional comparison can be drawn between the TPD profiles of the KUA-$CONH_2$ and KUA-NH_2 samples, Figure 6. As was observed by XPS, the amination reaction increases the amount of oxygen on the surface in the form of CO and CO_2-evolving groups. The CO_2 profile suggests the formation of carboxylic acids during the amination step, although direct comparison between the profiles of KUA-COOH and KUA-NH_2 (Figure 6a) confirms the overall consumption of carboxylic acids for the whole synthesis route. A possible explanation for the increase of CO_2-evolving groups in KUA-NH_2 is the esterification of lactams (that have been formed in the amidation step, Figure 4a), which can react with the methoxide present in the media and form esters that would subsequently be hydrolyzed to form again lactone moieties (reverted reaction of Figure 4a), evidencing that the Hofmann rearrangement to produce amines does not take place over lactams. This is supported by the loss of nitrogen detected by XPS after amination step (Table 2). This change also contributes to explain the larger apparent surface area and pore volume of KUA-NH_2 in comparison to KUA-$CONH_2$ (i.e. cyclic amides have a higher volume than the analogous oxygen rings, and therefore they are able to block a higher porosity amount). There have also been important changes in the CO evolution profile after the amination of KUA-$CONH_2$ sample, Figure 6b. If the low temperature region of both desorption profiles are compared, a decrease in the CO desorption related to amide decomposition (region between 200 and 400ºC) is observed for KUA-NH_2. This decrease is probably the consequence of a consumption of amides and lactams, which evidences the conversion of these groups into amines and lactones, respectively. This seems to be supported by the differences in the desorbed amount of nitrogen species in this region of temperatures in KUA-NH_2 (Figure 7b). Moreover, the sample KUA-NH_2 presents higher

amount of phenols (CO desorption at 600-700ºC) and a higher CO desorption at the end of TPD run (temperatures higher than 900ºC). The last one is produced simultaneously to the increase of the N-related signal recorded at high temperatures for KUA-NH_2, as shown in Figure 7b. This increase could be a consequence of a favored rearrangement or formation of N-containing aromatic rings (Figures 5b and 5c) during amination [30]. As for the CO increase, a favored insertion of hydroxyl groups during the amination treatment is possible due to the πdeficient behavior of pyridines, which facilitates nucleophilic substitution reactions on the adjacent carbon (Figure 4d). The resulting pyridones can be transformed into pyrroles by thermolysis, which produces the loss of a CO molecule, as is shown in Figure 5d [45]. This is supported by the XPS results obtained for the samples KUA-$CONH_2$ and KUA-NH_2 after the TPD treatment up to 950º C (Table 2), where the higher amount of pyrroles measured after TPD of KUA-NH_2 seems to be connected to the presence of a higher amount of pyridones in the original KUA-NH_2 sample.

3.3. Electrochemical characterization.

3.3.1. Cyclic Voltammetry

The pristine and modified materials have been characterized by cyclic voltammetry in the 0.2-0.8V potential range in 1M H_2SO_4 using different scan rates. Figure 8 shows the voltammograms for all activated carbon electrodes at low scan rate (1 mV/s). Gravimetric and surface capacitances (gravimetric capacitance divided by the BET surface area) are reported in Table 4. The formation of the electrical double layer is manifested in all of them, evidenced by the rectangular shape of their voltammograms between 0.2V and 0.65V. At high positive potentials an oxidation current is observed for all the samples and the oxidation current depends on the electrode material. The low scan rate used for the CV measurements provides enough time for ion diffusion into the pore network, so all the surface wetted by the electrolyte will be available for the formation of the double layer. The calculated capacitance is different for each material due to the differences in surface area and surface chemistry. However, it can be seen that the order in the values of the gravimetric capacitance (Table 4) does not follow in all the cases the trends observed in the BET surface area in Table 1. Thus, the activated carbon with the highest capacitance is the pristine carbon (KUA), but the highly oxidized KUA-COOH shows the lowest capacitance in spite of having higher surface area than KUA-$CONH_2$ and KUA-NH_2.

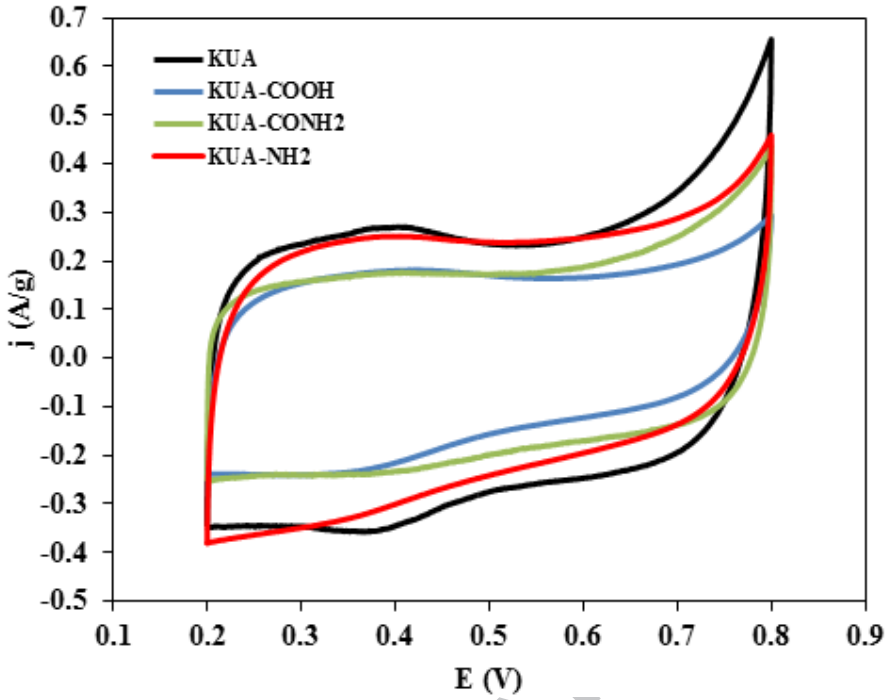

Figure 8. 2nd cyclic voltammograms in the potential range 0.2-0.8 V for KUA, KUA-COOH, KUA-$CONH_2$ and KUA-NH_2 electrodes.1M H_2SO_4. v=1 mV/s.

When capacitance is divided by BET surface area (i.e. surface capacitance, second column in Table 4), values concordant with those found in the literature for porous carbons are obtained [46], except for the one obtained for KUA-COOH. These results are an example of the influence of the surface chemistry in the electrochemical behavior of carbon materials. The effect of the surface oxygen groups in capacitance has been studied in previous works of our research group [24]. In general, oxygen functionalities improve the behavior of the electrodes mainly due to two effects: increase of wettability of the surface, which facilitates interactions with the electrolyte, and introduction of functional groups capable of experimenting redox reactions, generating pseudocapacitance [24,47]. These advantages are related to CO-desorbing groups, while the presence of CO_2-desorbing groups is unfavorable because of their electron-withdrawing properties that diminish the delocalization of the charge (and thereby the electrical conductivity). This effect explains the lower specific capacitance in KUA-COOH. However, the specific capacitance for KUA-$CONH_2$ is similar or even higher than for the other materials. In this sample, a significant part of the CO_2-desorbing groups are subsequently transformed into amides and derivatives, thus partially deactivating their negative influence, while keeping the positive influence coming for the presence of CO-desorbing [24] and other N-containing [48] groups.

Table 4. Gravimetric (Cg) and surface capacitances (Cg/S_{BET}) and Ohmic drop (IR_{drop}) for all the samples measured at different electrochemical conditions. 1 M H_2SO_4.

Sample	Cg [1mV/s] (F/g)	Cg/S_{BET} [1mV/s] (mF/m^2)	Cg [0.5 A/g] (F/g)	Cg [20 A/g] (F/g)	Cg [50 A/g] (F/g)	IR_{drop} [20 A/g] (mV)
KUA	299	95	268	82	33	106
KUA-COOH	171	64	138	6	3	380
KUA-$CONH_2$	217	105	206	125	82	66
KUA-NH_2	249	102	209	17	2	272

The impact of the changes in the surface chemistry in the capacitance retention was analyzed by recording CV at different scan rates, Figure 9. The pristine activated carbon is able to keep the CV characteristics up to 20 mV/s, while KUA-COOH and KUA-NH_2 yielded tilted voltammograms at scan rates of 10 mV/s and higher. In terms of capacitance retention, the three samples seem to behave similarly. Interestingly, the best results are obtained for the amidated sample (KUA-$CONH_2$) that is able to retain the CV shape up to 50 mV/s. Since the micropore size distribution seems to be similar for all the samples, as already discussed in section 3.1, these differences in behavior must be related to the changes in the surface chemistry of the samples.

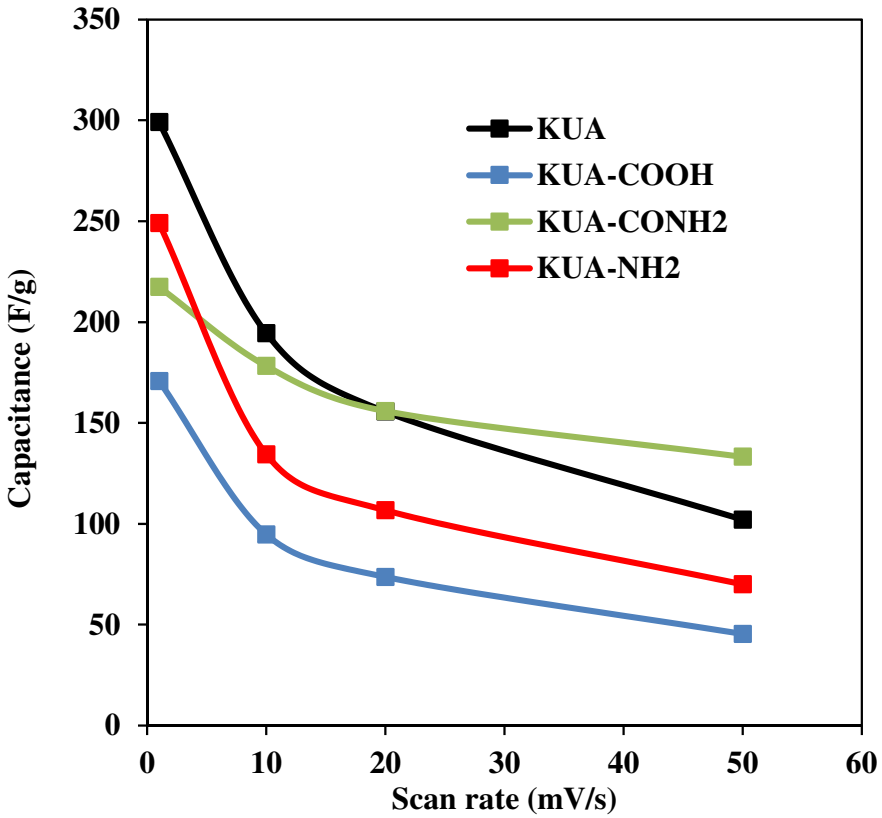

Figure 9. Gravimetric capacitance at different scan rates for KUA, KUA-COOH, KUA-$CONH_2$ and KUA-NH_2 electrodes.1M H_2SO_4. v= 1, 10, 20 and 50 mV/s.

The negative effect of surface oxygen groups and especially CO_2-desorbing groups in electrical conductivity can explain the low capacitance retention in KUA-COOH. KUA-NH_2 also has similar capacitance retention, but higher specific capacitance at all scan rates. In the case of KUA-$CONH_2$, the capacitance experiences the smaller decrease with scan rate, as proved in Figure 9. Consequently, this electrode has the highest specific capacitance at the highest tested scan rate. The capacitance retention capability is undoubtedly related to their surface chemistry, since it presents basically the same pore size distribution than the parent sample and the lowest specific surface area of the all studied materials. This effect has been studied in more detail using galvanostatic charge-discharge analyses.

3.3.2. Galvanostatic charge-discharge cycles

The rate performance of the original and the modified samples has been characterized by chronopotentiometry at different specific currents (from 0.05 to 50 A/g). Figure 10 shows the 4^{th} galvanostatic charge-discharge cycle at 0.5 A/g, 20 A/g and 50 A/g, and the obtained

capacitance and ohmic drop at 20 A/g are compiled in Table 4. The discharge time, which is directly related to the capacitance reported in Table 4, follows the order KUA>KUA-NH_2~KUA-$CONH_2$>KUA-COOH at 0.5 A/g. However, this tendency changes at higher specific currents (>10 A/g), being then KUA-$CONH_2$>>KUA>>KUA-NH_2>KUA-COOH. This result is in agreement with the capacitance values and capacitance retention observed in the cyclic voltammetry study, section 3.3.1. An outstanding capacitance value of 82 F/g was registered for the KUA-$CONH_2$ at 50 A/g, being high considering that it is achieved with a surface loading of 8 mg/cm^2, a value in the range of those used in the commercial formulation of supercapacitors [49].

The ohmic drop, reflected by the sudden drop in potential when moving from charge to discharge at 0.8V in Figures 10b and c, is also affected by the surface chemistry of the materials. This ohmic drop is associated to the electrical series resistance of the electrode, which includes the inherent resistance of the materials used in the different components of the cell (current collector, membrane, etc.), the interparticle electrical resistance (being connected to the electrode preparation), the intraparticle electrical resistance (which is related to the inherent conductivity of the sample) and the ion diffusional resistance (which depends on the pore size distribution and connectivity). Since the cell and the electrode preparation is identical in all the cases, and ion diffusional resistance must be similar for the analyzed materials, the important differences in the ohmic drop values must be related to the surface chemistry. As discussed before, the higher amount of CO_2-evolving groups results in a worse rate performance in KUA-COOH, while the presence of N functionalities in KUA-NH_2, which improve the wettability and electrical conductivity [6,8,48], seems to be responsible of its slightly better performance, although the behavior as supercapacitor electrode is still worse than the starting material, KUA. This is probably due to the lower amount of functional groups in KUA that facilitate the charge delocalization on its surface with respect to that of KUA-NH_2.

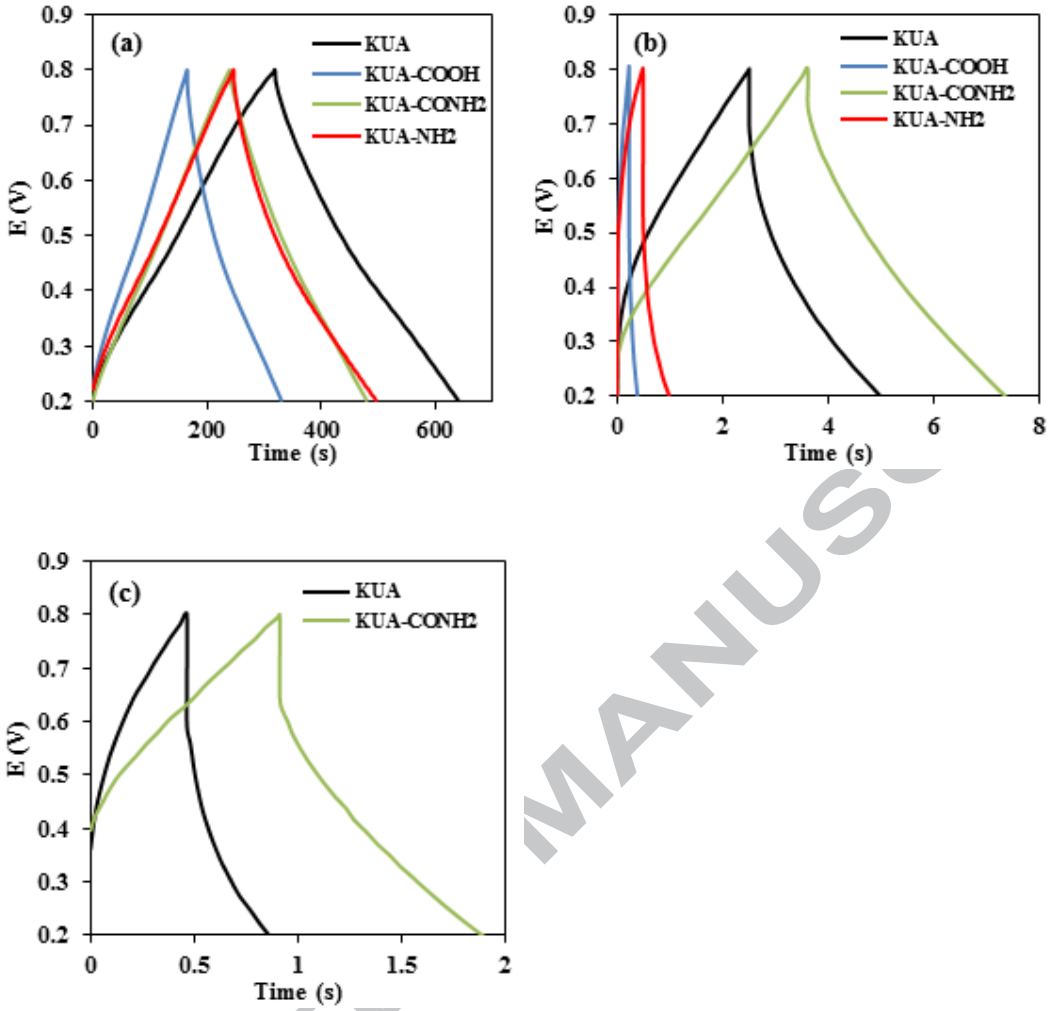

Figure 10. Galvanostatic charge-discharge curves at current densities of (a) 0.5 A/g, (b) 20 A/g and (c) 50 A/g. Potential range: 0.2-0.8V.

Very interestingly, the capacitance retention is greatly improved for the KUA-$CONH_2$ electrode, being much higher than that of the oxidized carbon KUA-COOH and even higher than that of the pristine activated carbon. Thus, the gravimetric capacitance of KUA-$CONH_2$ is higher than that found for KUA at specific currents higher than 10 A/g, thanks to the lower ohmic drop found for this material (Table 4). This material seems to behave similar in terms of capacitance retention than other N-containing porous carbon materials prepared from N-containing precursors reported in literature [4,6,50-54]. Other N-doping techniques, such as ammoxidation or urea treatment [55,56], do not seem to produce such a good capacitance retention as the amidation route proposed in this work.

The mechanism behind the capacitance and the electrical conductivity improvement in N-containing carbon materials is still under debate in the literature [6-8,11,57-59]. Theoretical studies [59] have proven that the nitrogen of pyrrole groups improves the electron mobility of the carbon matrix through introduction of electron-donor properties and increases the catalytic activity of the carbon in electron transfer reactions. Also, the nitrogen atoms present in a six member ring in the edge of a graphene layer can be considered as pyrrole-like functionalities due to the conjugation of its two p electrons with the π system of the graphene layer. Hulicova-Hurkacova and coworkers indicated that lactams and imides can be considered as pyrrole-like groups, since they present both characteristics [6]; also, they proposed the participation of nitrogen and oxygen of imide, lactam and pyridone groups in pseudocapacitance processes. This explains the high capacitance retention of the electrode KUA-$CONH_2$, which presents a higher amount of pyrrole-like groups on its surface. On the other hand, they rejected the participation of amine and amide groups in the improvement of electro-donating properties. However, we consider that the presence of amides can also improve the behavior of the sample KUA-$CONH_2$, because part of the carboxylic acids that were present on the surface of KUA-COOH has been replaced and, although amides are also electron-withdrawing groups, when they are attached to the aromatic ring through the carbonyl group, this character is lower than that of carboxylic acids. Also, Hsieh and coworkers [11] indicated the possible contribution of amide groups in pseudocapacitive processes in supercapacitors of CNTs modified by a synthetic path quite similar to our approach. Finally, the benefits of pyridines in carbon material with respect to electrical conductivity is unclear, whereas its positive influence in capacitance seems to be associated with enhanced wettability [57], enhanced interaction with ions [58] and the occurrence of pseudofaradaic processes[57], which is reported to take place through the following reaction [60]:

$$HC{=}N + H_2O \leftrightarrow CHN{=}O + 2e^- + 2H^+$$

In a different work about the effect of nitrogen functionalities in the electrochemical behavior of carbon materials [8], the contribution of pyridines in the surface of nitrogen-containing CNTs to the enhancement of capacitance was found to be higher in basic electrolyte, so its presence is not expected to be critical in the behavior of the materials studied in this work at acidic conditions.

Hence, the improvements in the capacitance retention found in KUA-$CONH_2$ can be explained by the lower amount of carboxylic acids in the surface when compared to KUA-NH_2 (Figure 6) and by the nitrogen functional groups on its surface. Since the main differences in the chemical composition in terms of nitrogen surface groups between KUA-$CONH_2$ and KUA-NH_2 is the presence of amide groups and derivatives in the former that have been replaced by amines and carboxylic acids in the latter, and considering that amines have a higher electron-donating character than amides, the enhanced performance of the KUA-$CONH_2$ is attributable to the cyclic amides (lactams and imides) and their pyrrol-like effect on the electrochemical performance of carbon electrodes [6].

4. Conclusions

Functionalization of activated carbon using an organic chemistry protocol has been carried out by amidation treatment and Hofmann rearrangement. Nitrogen content of about 3 at% is achieved through this process under mild conditions. As consequence of the heterogeneous surface chemistry of activated carbons, a wide range of functional groups have been produced onto the surface of the modified samples, showing different nitrogen and oxygen functional groups on KUA-$CONH_2$ and KUA-NH_2. The amidation treatment produces amides (and cyclic derivatives, such as imides and lactams) on KUA-$CONH_2$, but the presence of CO-desorbing groups on KUA-COOH yields the generation of nitrogen aromatic heterocycles (pyridine, pyridone and pyrrole). Consequently, KUA-$CONH_2$ presents a complex surface chemistry with different nitrogen functional groups, some of them also stable at high temperatures (pyrrole and pyridine). The post-treatment by Hofmann rearrangement produces the conversion of amides into amines, obtaining an activated carbon (KUA-NH_2) with different nitrogen functionalities (amines, pyridines and pyrroles) and a high amount of surface oxygen groups. Different reaction pathways are proposed to explain the observed changes.

The different surface chemistry of all activated carbons allows us to study its effect on their electrochemical performance. At low current densities, the capacitance is mainly governed by the apparent surface area while the specific capacitance is greater for the N-containing samples, evidencing the influence of nitrogen functional groups. Interestingly, KUA-$CONH_2$ showed the highest capacitance retention, keeping an outstanding value of 83 F/g at 50 A/g, a value especially high considering the electrode thickness. This capacitance retention was not registered for any of the other electrodes and, therefore, it might be due to the lower amount

of electron-withdrawing groups, as carboxylic acids, and to the nitrogen functional groups existing on KUA-$CONH_2$, such as pyridines, cyclic amides (lactams and imides) and pyrroles, which improve the charge delocalization and thereby increase the electrical conductivity.

Acknowledgements

This work was supported by the Ministry of Economy and competitiveness of Spain (MINECO) and FEDER (CTQ2012-31762, MAT2013-42007-P) and Generalitat Valenciana (PROMETEO/2013/038 and PROMETEOII/2014/010). RRR thanks MINECO for 'Juan de la Cierva' contract (JCI-2012-12664).

References

[1] Bandosz TJ, Ania CO. Surface chemistry of activated carbons and its characterization. In: Bandosz TJ, editor. Activated Carbon Surfaces in Environmental Remediation, New York:1st ed, Elsevier; 2006, p. 159–229.

[2] Bandosz TJ. Surface Chemistry of Carbon Materials. In: Serp P, Figueiredo JL, editors. Carbon Materials for Catalysis, John Wiley & Sons, Inc; 2009, p. 45–92.

[3] Radovic LR. Surface Chemical and Electrochemical Properties of Carbons. In: Beguin F, Frackowiak E, editors. Carbons for Electrochemical Energy Storage and Conversion Systems, Boca Raton, FL: Taylor & Francis (CRC Press); 2010, p. 163–219.

[4] Shen W, Fan W. Nitrogen-containing porous carbons: synthesis and application. J Mater Chem A 2013;1(4): 999-1013.

[5] Gong KP, Du F, Xia ZH, Durstock M, Dai LM. Nitrogen-doped carbon nanotube arrays with high electrocatalytic activity for oxygen reduction. Science 2009;323:760–4.

[6] Hulicova-Jurcakova D, Kodama M, Shiraishi S, Hatori H, Zhu ZH, Lu GQ. Nitrogen-enriched nonporous carbon electrodes with extraordinary supercapacitance. Adv Funct Mater 2009;19(11):1800–9.

[7] Salinas-Torres D, Shiraishi S, Morallón E, Cazorla-Amorós D. Improvement of carbon materials performance by nitrogen functional groups in electrochemical capacitors in organic electrolyte at severe conditions. Carbon 2015;82:205-13.

[8] Ornelas O, Sieben JM, Ruiz-Rosas R , Morallón E, Cazorla-Amorós D, Geng J, et al. On the origin of the high capacitance of nitrogen-containing carbon nanotubes in acidic and alkaline electrolytes. Chem Commun 2014;50:11343-6.

[9] Raymundo-Piñero E, Cazorla-Amorós D, Linares-Solano A. The role of different nitrogen functional groups on the removal of SO_2 from flue gases by N-doped activated carbon powders and fibres. Carbon 2003;41(10):1925–32.

[10] Sevilla M, Valle-Vigón P, Fuertes AB. N-Doped polypyrrole-based porous carbons for CO_2 capture. Adv Func Mater 2011;21(14):2781–7.

[11] Hsieh C-T, Teng H, Chen W-Y, Cheng Y-S. Synthesis, characterization, and electrochemical capacitance of amino-functionalized carbon nanotube/carbon paper electrodes. Carbon 2010;48(15):4219–29.

[12] Silva AR, Martins M, Freitas MM, Valente A, Freire C, de Castro B, et al. Immobilisation of amine-functionalised nickel(II) Schiff base complexes onto activated carbon treated with thionyl chloride. Microporous Mesoporous Mater 2002;55(3):275–84.

[13] Silva AR, Martins M, Freitas MMA, Figueiredo JL, Freire C, de Castro B. Anchoring of copper(II) acetylacetonate onto an activated carbon functionalised with a triamine. Eur J Inorg Chem 2004;10:2027–35.

[14] Silva AR, Budarin V, Clark JH, Freire C, de Castro B. Organo-functionalized activated carbons as supports for the covalent attachment of a chiral manganese(III) salen complex. Carbon 2007;45(10):1951–64.

[15] Alves JAC, Freire C, de Castro B, Figueiredo JL. Anchoring of organic molecules onto activated carbon. Colloids Surf A 2001;189(1-3):75–84.

[16] Tamai H, Shiraki K, Shiono T, Yasuda H. Surface functionalization of mesoporous and microporous activated carbons by immobilization of diamine. J Colloid Interface Sci 2006;295(1):299–302.

[17] Peñas-Sanjuán A, López-Garzón R, Domingo-García M, López-Garzón FJ, Melguizo M, Pérez-Mendoza M. An efficient procedure to bond nanostructured nitrogen functionalities to carbon surfaces. Carbon 2012;50(11):3977–86.

[18] El-Sayed Y, Bandosz TJ. Role of surface oxygen groups in incorporation of nitrogen to activated carbons via ethylmethylamine adsorption. Langmuir 2005;21(4):1282–9.

[19] Abe M, Kawashima K, Kozawa K, Sakai H, Kaneko K. Amination of activated carbon and adsorption characteristics of its aminated surface. Langmuir 2000;16(11):5059–63.

[20] Gromov A, Dittmer S, Svensson J, Nerushev OA, Perez-García SA, Licea-Jiménez L, et al. Covalent amino-functionalisation of single-wall carbon nanotubes. J Mater Chem 2005;15:3334–9.

[21] Lozano-Castelló D, Lillo-Ródenas MA, Cazorla-Amorós D, Linares-Solano A. Preparation of activated carbons from Spanish anthracite. I Activation by KOH. Carbon 2001;39(5):741–9.

[22] Boehm HP. Surface oxides on carbon and their analysis: a critical assessment. Carbon 2002;40(2):145–9.

[23] Moreno-Castilla C, López-Ramón MV, Carrasco-Marín F. Changes in surface chemistry of activated carbons by wet oxidation. Carbon 2000;38(14):1995–2001.

[24] Bleda-Martínez MJ, Lozano-Castelló D, Morallón E, Cazorla-Amorós D, Linares-Solano A. Chemical and electrochemical characterization of porous carbon materials. Carbon 2006;44(13):2642–51.

[25] Willocq C, Hermans S, Devillers M. Active carbon functionalized with chelating phosphine groups for the grafting of model Ru and Pd coordination compounds. J Phys Chem C 2008;112(14):5533–41.

[26] Jeong YN, Choi MY, Choi HC. Preparation of Pt- and Pd- decorated CNTs by DCC-activated amidation and investigation of their electrocatalytic activities. Electrochim Acta 2012; 60: 78-84.

[27] Cazorla-Amorós D, Alcañiz-Monge J, de la Casa-Lillo MA, Linares-Solano A. CO_2 as an adsorptive to characterize carbon molecular sieves and activated carbons. Langmuir 1998;14(16):4589–96.

[28] Raymundo-Piñero E, Cazorla-Amorós D, Linares-Solano A, Find J, Wild U, Schlögl R. Structural characterization of N-containing activated carbon fibers prepared from a low softening point petroleum pitch and a melamine resin. Carbon 2002;40(4):597–608.

[29] Biniak S, Szymański G, Siedlewski J, Świa Tkowski A. The characterization of activated carbons with oxygen and nitrogen surface groups. Carbon 1997;35(12):1799–810.

[30] Jansen RJJ, van Bekkum H. XPS of nitrogen-containing functional groups on activated carbon. Carbon 1995;33(8):1021–7.

[31] Kapteijn F, Moulijn JA., Matzner S, Boehm HP. The development of nitrogen functionality in model chars during gasification in CO_2 and O_2. Carbon 1999;37(7):1143–50.

[32] Yamada Y, Kim J, Matsuo S, Sato S. Nitrogen-containing graphene analyzed by X-ray photoelectron spectroscopy. Carbon 2014;70:59–74.

[33] Smith MB, March J. March's Advanced Organic Chemistry: Reaction, Mechanisms and Estructure. 6th ed. Hoboken, New Jersey, USA: John Wiley & Sons, Inc. 2007: 1429–30.

[34] Smith MB, March J. March's Advanced Organic Chemistry: Reaction, Mechanisms and Estructure. 6th ed. Hoboken, New Jersey, USA: John Wiley & Sons, Inc. 2007: 1436.

[35] Clayden J, Greeves N, Warren S, Wothers P. Organic Chemistry. 1st ed. Oxford University Press. 2001: 1150–1.

[36] Smith MB, March J. March's Advanced Organic Chemistry: Reaction, Mechanisms and Estructure. 6th ed. Hoboken, New Jersey, USA: John Wiley & Sons, Inc. 2007: 1281–4.

[37] Clayden J, Greeves N, Warren S, Wothers P. Organic Chemistry. 1st ed. Oxford University Press. 2001: 349–51.

[38] Clayden J, Greeves N, Warren S, Wothers P. Organic Chemistry. 1st ed. Oxford University Press. 2001: 1186–7.

[39] Smith MB, March J. March's Advanced Organic Chemistry: Reaction, Mechanisms and Estructure. 6th ed., Hoboken, New Jersey, USA: John Wiley & Sons, Inc. 2007: 1263–7.

[40] Román-Martínez MC, Cazorla-Amorós D, Linares-Solano A, Salinas-Martínez de Lecea C. Tpd and TPR characterization of carbonaceous supports and Pt/C catalysts. Carbon 1993;31(6):895–902.

[41] Lopez-Ramon MV, Stoeckli F, Moreno-Castilla C, Carrasco-Marin F. On the characterization of acidic and basic surface sites on carbons by various techniques. Carbon 1999;37(8):1215–21.

[42] Figueiredo JL, Pereira MFR, Freitas MMA, Órfão JJ. Modification of the surface chemistry of activated carbons. Carbon 1999;37(9):1379–89.

[43] Bleda-Martínez MJ, Maciá-Agulló JA, Lozano-Castelló D, Morallón E, Cazorla-Amorós D, Linares-Solano A. Role of surface chemistry on electric double layer capacitance of carbon materials. Carbon 2005;43(13):2677–84.

[44] Moreno-Castilla C, Ferro-García MA, Joly JP, Bautista-Toledo I, Carrasco-Marín F, Rivera-Utrilla J. Activated carbon surface modifications by nitric acid, hydrogen peroxide, and ammonium peroxydisulfate treatments. Langmuir 1995;11(11):4386–92.

[45] Schmiers H, Friebel J, Streubel P, Hesse R, Kopsel R. Change of chemical bonding of nitrogen of polymeric N - heterocyclic compounds during pyrolysis. Carbon 1999;37(12):1965–78.

[46] Qu D. Studies of the activated carbons used in double-layer supercapacitors. J Power Sources 2002;109(2):403–11.

[47] Conway BE, Birss V, Wojtowicz J. The role and utilization of pseudocapacitance for energy storage by supercapacitors. J Power Sources 1997;66(1-2):1–14.

[48] Lota G, Grzyb B, Machnikowska H, Machnikowski J, Frackowiak E. Effect of nitrogen in carbon electrode on the supercapacitor performance. Chem Phys Lett 2005;404(1-3):53–8.

[49] Stoller MD, Ruoff RS. Best practice methods for determining an electrode material's performance for ultracapacitors. Energy Environ Sci 2010;3:1294-301.

[50] Alabadi A, Yang X, Dong Z, Tan B. Nitrogen-doped activated carbons derived from a co-polymer for high supercapacitor performance. J Mater Chem A 2014;2:11697–705.

[51] Paraknowitsch JP, Zhang J, Su D, Thomas A, Antonietti M. Ionic liquids as precursors for nitrogen-doped graphitic carbon. Adv Mater 2010;22(1):87–92.

[52] Kim K-S, Park S-J. Synthesis and high electrochemical capacitance of N-doped microporous carbon/carbon nanotubes for supercapacitor. J Electroanal Chem 2012;673:58–64.

[53] Wu C, Wang X, Ju B, Jiang L, Wu H, Zhao Q, et al. Supercapacitive performance of nitrogen-enriched carbons from carbonization of polyaniline/activated mesocarbon microbeads. J Power Sources 2013;227:1–7.

[54] Wickramaratne NP, Xu J, Wang M, Zhu L, Dai L, Jaroniec M. Nitrogen enriched porous carbon spheres: attractive materials for supercapacitor electrodes and CO_2 adsorption. Chem Mater 2014;26(9):2820–8.

[55] Pietrzak R, Jurewicz K, Nowicki P, Babeł K, Wachowska H. Microporous activated carbons from ammoxidised anthracite and their capacitance behaviours. Fuel 2007;86(7-8):1086–92.

[56] Jurewicz K, Pietrzak R, Nowicki P, Wachowska H. Capacitance behaviour of brown coal based active carbon modified through chemical reaction with urea. Electrochim Acta 2008;53(16):5469–75.

[57] Seredych M, Hulicova-Jurcakova D, Lu GQ, Bandosz TJ. Surface functional groups of carbons and the effects of their chemical character, density and accessibility to ions on electrochemical performance. Carbon 2008;46(11):1475–88.

[58] Jeong HM, Lee JW, Shin WH, Choi YJ, Shin HJ, Kang JK, et al. Nitrogen-doped graphene for high-performance ultracapacitors and the importance of nitrogen-doped sites at basal planes. Nano Lett 2011;11(2):2472–7.

[59] Strelko VV, Kuts VS, Thrower PA. On the mechanism of possible influence of heteroatoms of nitrogen, boron and phosphorus in a carbon matrix on the catalytic activity of carbons in electron transfer reactions. Carbon 2000;38(10):1499–503.

[60] Frackowiak E, Lota G, Machnikowski J, Vix-Guterl C, Béguin F. Optimisation of supercapacitors using carbons with controlled nanotexture and nitrogen content. Electrochim Acta 2006;51(11):2209–14.